arXiv:1207.5311v1 [cond-mat.mes-hall] 23 Jul 2012

All-optical control of the spontaneous emission of quantum dots using coupled-cavity quantum electrodynamics

C. Y. Jin *,[1] M. Y. Swinkels †,[1] R. Johne †,[1] T. B. Hoang,[1] L. Midolo,[1] P. J. van Veldhoven,[1] and A. Fiore[1]

[1] *COBRA Research Institute, Eindhoven University of Technology,*
P.O.Box 513, 5600MB Eindhoven, the Netherlands

(Dated: July 24, 2012)

We demonstrate the remote all-optical control of the spontaneous emission (SE) of quantum dots using coupled photonic crystal cavities. By spectrally tuning a Fabry-Perot cavity in resonance with a target cavity, the quality factor and the local density of states experienced by emitters in the target cavity are modified, leading to a change in the SE rate. From the theoretical analysis of the coupled-cavity quantum electrodynamics system, the SE rate change can be higher than the quality factor change due to a reduction of the vacuum field at the emitter's position when the two cavities are brought in resonance. Both the weak and strong coupling regimes of two cavities have been observed experimentally and the SE decay rate has been modified by more than a factor of three with remote optical control.

Photonic crystal (PhC) cavities with a small mode volume and a high quality factor (Q-factor) represent an ideal experimental platform for solid-state cavity quantum electrodynamics (CQED) [1, 2]. Semiconductor quantum dots (QDs), precisely positioned inside PhC cavities, are anticipated to serve as scalable quantum emitters and nodes for future quantum information processing and quantum computing systems [3, 4]. In an ideal quantum node, quantum information should be stored in the charge or spin degree of freedom of a solid-state quantum system, and then released to a photonic channel, e.g. by spontaneous emission (SE). The SE rate and its coupling efficiency to a given optical mode can be greatly enhanced by controlling the local density of states (LDOS) at the emitter's position using a wavelength-sized, low-loss cavity [5, 6]. In order to control the timing of the emission process, a procedure is needed to switch the emitter-cavity coupling on and off on the pico-second (ps) time scale. An attractive approach is the ultrafast control of the cavity characteristics, leading to a dynamic modulation of the LDOS and therefore of the SE rate. The dynamic tuning of the Q-factor recently demonstrated in silicon-based PhC cavities is an example of such ultrafast cavity modulation techniques [7, 8]. However, their application to CQED requires a remote control scheme which produces large changes in the LDOS but does not affect the emitter-cavity interaction by a local perturbation. A static and quasi-permanent change of the Q-factor and of the emission intensity of QDs was recently demonstrated by producing a structural modification in the vicinity of the cavity [9]. The coupled-cavity quantum electrodynamics (CCQED) platform proposed by Hughes [10] is an interesting candidate for the control of the SE rate: When two distant cavities are optically coupled, modifications to one cavity affect the coupled modes and therefore the LDOS seen by an emitter in the other cavity. Several demonstrations of strong coupling between PhC cavities have been reported recently [11–13]. In this work we report the experimental observation of the controlled and reversible modification of the SE rate in a "target" cavity by tuning the properties of a remote "control" cavity. The tuning is implemented using thermo-optic effects, but the concept is readily extendable to the ps time scale by using free-carrier injection, opening the way to the dynamic control of SE in solid-state cavities.

Fig. 1 (a) shows an ideal atom-cavity scheme where one of the cavity mirrors is replaced by a Fabry-Perot (FP) etalon. The FP cavity mode has a periodic mode structure sketched in Fig. 1 (b) and it is assumed to have a lower Q-factor compared to the target cavity mode. By adjusting the length of the FP cavity or modulating the refractive index of the media inside it, the set of FP modes can be spectrally tuned with respect to the target cavity mode. At resonance the coupling causes an additional leakage for the optical field confined in the target cavity resulting in a reduction of the Q-factor. The SE rate of an emitter in the target cavity can be controlled non-locally by adjusting the resonant condition.

The SE enhancement of a two-level system in a cavity mode is typically described in perturbation theory by the Purcell factor F, [5, 14]

$$F = \frac{3}{4\pi^2}\left(\frac{\lambda}{n_r}\right)^3 Q\left|\mathbf{E}(\mathbf{r_0})\right|^2 \tag{1}$$

where λ is the cavity wavelength, n_r is the refractive index, Q is the Q-factor of the cavity mode and $\mathbf{E}(\mathbf{r_0})$ is the normalized mode function at the dipole position $\mathbf{r_0}$. The SE enhancement is therefore governed by the change in Q-factor and in the mode function distribution.

The presented system can be described by a threeoscillator model including the dipole, the target cavity, the FP cavity, and the coupling terms between them. The dressed states of the system can be obtained by diagonalizing the non-Hermitian Hamiltonian [15]

---

*Electronic mail: c.jin@tue.nl

†These two authors contributed equally to this work

$$H = \hbar \begin{bmatrix} \omega_0 + i\gamma_0 & g & 0 \\ g & \omega_t + i\kappa_t & \eta \\ 0 & \eta & \omega_{FP} + i\kappa_{FP} \end{bmatrix} \quad (2)$$

where ω_0, ω_t and ω_{FP} denote the angular frequencies of the dipole, the target cavity mode and the FP cavity mode, and η is the coupling rate between the two cavities. The coupling rate between the dipole and the target cavity is described by g, and weak coupling ($g \ll \kappa_t, \kappa_{FP}$) is assumed for the following theory and experiments. The dipole is placed in the target cavity and thus is spatially decoupled from the FP modes. We first solve the subsystem of coupled cavities, which yields the eigenvalues

$$\begin{aligned} \omega_{1,2} =& \frac{(\omega_t + i\kappa_t) + (\omega_{FP} + i\kappa_{FP})}{2} \\ & \pm \frac{1}{2}\sqrt{((\omega_t + i\kappa_t) - (\omega_{FP} + i\kappa_{FP}))^2 + 4\eta^2}. \end{aligned} \quad (3)$$

The effect of wavelength detuning $\lambda_c - \lambda_{FP}$ on the Q factor of the coupled cavity modes is illustrated in Fig. 1 (c). By tuning a low Q cavity mode through a high Q target cavity mode a significant change in the imaginary parts of the coupled eigenfrequencies $\mathtt{Im}(\omega_{1,2})$ hence in the Q-factor can be observed at the crossing point.

Transforming the matrix (2) into the basis of the coupled cavity modes in Eq. 3 yields

$$H' = \hbar \begin{bmatrix} \omega_0 + i\gamma_0 & \alpha^* g & -\beta^* g \\ \alpha g & \omega_1 & 0 \\ -\beta g & 0 & \omega_2 \end{bmatrix}. \quad (4)$$

The normalized mode functions, $\mathbf{E_{1,2}(r)}$, of the coupled-cavity system are mixtures of the eigenfunctions of the initial cavity modes, $\mathbf{E}_{1,2}(\mathbf{r}) = \alpha_{1,2}\mathbf{E}_t(\mathbf{r}) + \beta_{1,2}\mathbf{E}_{FP}(\mathbf{r})$, where $\alpha_1 = \beta_2 = \alpha$, $\alpha_2 = -\beta_1 = \beta$, and $|\alpha|^2 + |\beta|^2 = 1$. Consequently, the coupling constants between the dipole and the new eigenmodes are weighted by their target cavity fraction due to the positioning of the dipole. Because of the mode coupling, the mode distribution of the state ω_1 becomes increasingly delocalized for decreasing detuning, leading to a reduction of the vacuum field at the dipole's position. This effect can be intuitively interpreted as a change of the effective mode volume due to the field delocalization.

The modulation of the Q-factors and of the coupling constants will affect the dynamics of the dipole-cavity interaction. For instance in the case that the two coupled cavities are in the strong coupling regime ($\eta \gg \kappa_c, \kappa_{FP}$), due to the energy splitting a narrow dipole will interact with only one of the two eigenmodes, leading to $F_1 \cong |\alpha|^2 \dfrac{Q_1}{Q_t} F_t = \dfrac{1}{2}\dfrac{Q_1}{Q_t} F_t$ when the two cavities are resonant. It follows that the Purcell factor is not only affected by the Q-change but also reduced by a factor of two due to the mode delocalization. In contrast, in the weak coupling case ($\eta \ll \kappa_c, \kappa_{FP}$), the SE enhancement has contributions from both coupled modes $F \cong |\alpha|^2 \dfrac{Q_1}{Q_t} F_t + |\beta|^2 \dfrac{Q_2}{Q_t} F_t$, which yields $F \cong F_t$ in the case of $Q_2 = Q_1$.

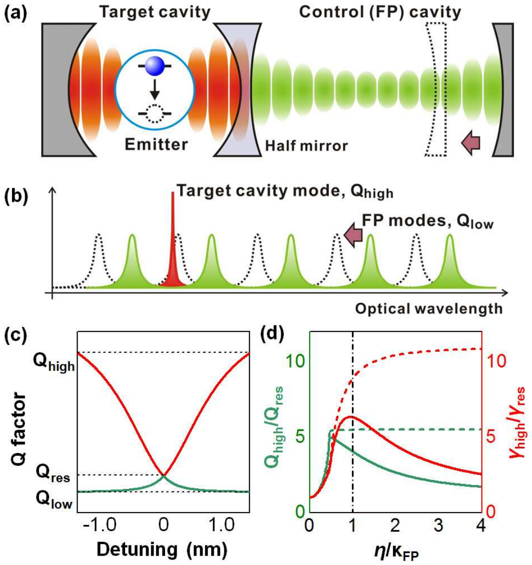

FIG. 1: (a) A schematic picture of a CCQED system. An emitter is placed in the target cavity with a higher Q-factor. A control cavity (FP cavity) which has periodic modes with lower Q-factors is optically coupled to the target cavity through a semitransparent mirror. (b) By controlling the effective cavity length of the FP cavity, FP modes can be tuned in resonance with the target cavity mode. (c) Calculated Q-factors for the coupled modes in the strong coupling regime as a function of the wavelength detuning between the original cavity modes. (d) Calculated Q-factor change (green curves) and the SE rate change (red curves) as a function of the normalized coupling strength. Dashed curves are for the ideal case of a single FP mode and solid curves take into account multiple FP modes.

Fig. 1 (d) presents simulation results for the CCQED system using matrix (2) [16]. The ratio between the initially uncoupled Q-factor and the Q-factor at resonance, Q_{high}/Q_{res}, is plotted as a function of the coupling strength divided by the FP cavity loss, η/κ_{FP}. The corresponding SE decay rate ratio, $\gamma_{high}/\gamma_{res}$ of the dipole as a function of the coupling strength is also plotted. While in the weak coupling regime the SE enhancement follows the change in the Q-factor, in the strong coupling regime the SE enhancement is a factor of two different from the Q-change as discussed above. In a realistic system, the FP cavity shows multiple and equally

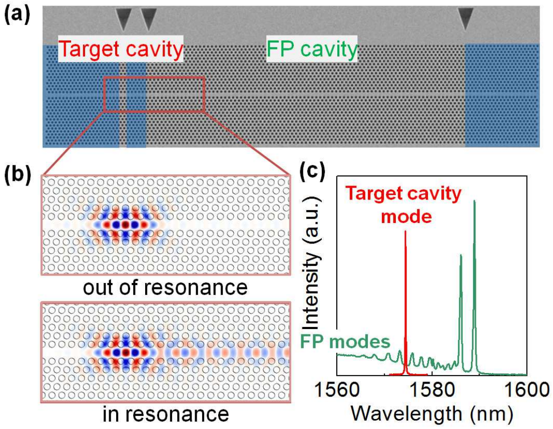

FIG. 2: (a) A SEM image of the fabricated PhC cavities. Three blue-shadowed squares indicate the barriers of waveguide cavities. (b) Simulated electrical field (y-polarized, E_y) distribution between two cavities when they are out of resonance (top) and in resonance (bottom). (c) μPL spectra of CCQED system when focusing the excitation beam on the target cavity (red) and FP cavity (green).

spaced resonances and the target cavity mode can couple to more than one FP mode simultaneously in case of high coupling strength, which modifies the Q-factor change and the SE change of the dipole, as shown by the green and red solid curves in Fig. 1(d).

In the experiment, our platform for the CCQED is based on PhC cavities using QDs as the emitter. Cavities were realized within a hexagonal PhC lattice fabricated in an InGaAsP membrane which contains a single layer of self-assembled InAs QDs with a dot density around $2 \times 10^9 cm^{-2}$. The QD ensemble gives a broad emission centered at 1570nm [17]. Fig. 2 (a) shows the scanning electron microscope (SEM) image of the fabricated structure based on two local defects along a W1 PhC waveguide. The target cavity is constituted by a high-Q double-heterostructure (DHS) cavity [18] with two periods of the lattice constant slightly larger than the original lattice constant, $a_1 = 1.03 \times a_0$. The FP cavity consists of eighty periods of modulated lattice constant ($a_2 = a_1$). Fig. 2 (b) presents the simulated electric field distribution based on 3D FDTD method [19]. A leakage from the target cavity to the FP cavity can be clearly observed when the two cavities are in resonance. The measurements were performed in a confocal microscope at a temperature of 77 K, in order to reduce the influence from the non-radiative recombination and the homogenous broadening of QDs, while allowing the thermo-optic tuning of the PhC cavity [20]. A diode laser emitting at 780 nm was used for exciting the cavity and the μPL singnal collected by the objective is measured with a spectrometer and an InGaAs array. Fig. 2(c) shows two typical μPL spectra taken from single-beam measurements by focusing the laser beam on either the target or FP cavity. The FP cavity has a quasi-periodic mode structure, which is governed by the modified dispersion relation close to the slow-light frequency of the PhC waveguide [21].

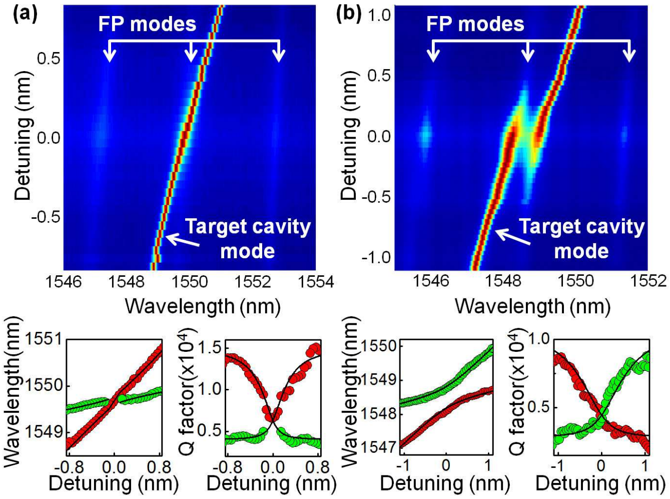

FIG. 3: (a) Weak and (b) strong coupling between two PhC cavities in a single-beam measurement on the target cavity. The continuous black lines are fits based on the coupled mode theory.

Firstly, single-beam measurements have been performed with one laser beam focused on the target cavity and the signal collected from the same position. By increasing the laser power, a red shift of the target cavity mode due to thermo-optic tuning is observed with only a small shift of FP modes caused by heat diffusion [13]. Fig. 3(a) shows a weak coupling case in a PhC with 4.5-period barrier between two cavities and 20-period barriers on the two sides. The main panel in Fig. 3(a) shows the spectral map with normalized intensities for various detunings, while the two small plots present the cavity mode wavelength and Q-factor as functions of the wavelength detuning. It exhibits a clear crossing of two coupled modes and indicates the weak coupling regime. The Q-factor of the target cavity decreases down from 13800 to 6500 and then increases again to 15100, whilst the Q-factor of the FP cavity increases slightly from 4000 to 4900 and then decreases to 3500. By fitting the crossing behavior of two coupled modes using Eq. 3, as shown by the black lines, we extract the parameters $Q_t = 1.5 \times 10^4$, $Q_{FP} = 4 \times 10^3$, and $\eta = 0.8 \times \kappa_{FP}$. Fig. 3(b) exhibits a different situation where the barrier thickness between two cavities is reduced to 4 periods. In this case, two coupled modes shows anti-crossing, which indicates the strong coupling regime. The Q-factor of the mode at shorter (longer) wavelength varies from 8500 to 1800 (from 2600 to 8500), respectively. Numerical fitting reveals $Q_t = 1.1 \times 10^4$, $Q_{FP} = 2.5 \times 10^3$, and $\eta = 1.1 \times \kappa_{FP}$.

Two-beam measurements have been carried out to demonstrate the remote control of both Q-factor and SE rate with one pulsed laser beam ($\lambda = 750nm$, pulse width

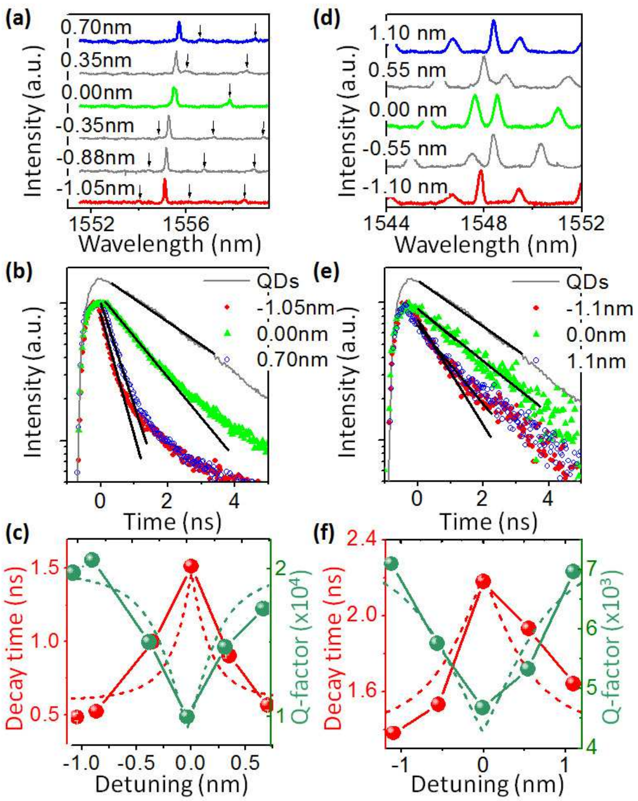

FIG. 4: Remote control of the Q factor and SE rate using two beam measurement for a weak coupling case (a-c) and a strong coupling case (d-f). (a) and (d). μPL spectra measured at different wavelength detuning. (b) and (e). SE decay curves at different wavelength detuning. The grey curve is the SE decay from QDs in the bulk. (c) and (f). The decay time and Q-factor at the high-Q mode as a function of the wavelength detuning. The dashed curves are simulations based on the coupled mode theory.

100 ps) focused on the target cavity and a CW heating laser beam focused at the center of the FP cavity, which is tilted slightly of the optical axis of the objective lens in order to position it at a distance of a few tens of micrometers from the other beam. Fig. 4(a) presents the spectra with weakly-coupled cavities at different pump powers of the tuning laser. The decay time of QDs resonant with the high-Q coupled mode has been measured by time-correlated single photon counting with a superconducting single photon detector [22], using a narrow bandpass filter ($\Delta\lambda = 0.5nm$). Fig. 4(b) shows the SE decay at the high-Q mode frequency with different wavelength detunings between the cavities and the decay of the QD emission in the bulk (outside the PhC), in a $\Delta\lambda = 20nm$ bandwidth, as a reference (grey curve). By fitting the initial part of the curve with an exponential decay function, the spontaneous emission lifetime modulated by PhCs is obtained, while the slow decay component is attributed to dark excitons [23]. Compared to the 2.5 ns decay time of the QD emission, the decay time at target cavity is 0.5 ns and 1.5 ns when two weakly coupled modes are off-resonance and in resonance, respectively. The strong coupling case has been also studied as shown in Fig. 4(d)-(f). The SE decay time is 1.4 and 2.2 ns for the high-Q mode, when two cavity modes are out of and in resonance, respectively.

To fit the experimental decay times we use the expression $\gamma^{exp} = \gamma_{cav}^{theor} + \gamma_{leak}$, where γ_{cav}^{theor} is the total emission rate into the two coupled modes calculated from diagonalizing the matrix (2), while $\gamma_{leak} = (3.1ns)^{-1}$ is the emission rate into the out-of-plane leaky modes which is measured from the decay time of QDs in the PhC mirror region. The global fit as shown by the dashed curves in Fig. 4(c) and (f) closely matches the experimental results. $\eta/\kappa_{FP} = 0.95$ and 1.40 can be identified for the weak and strong coupling, respectively. Both are close to the transition regime defined by $\eta/\kappa_{FP} = 1$. The measured decay rate into the cavity modes changes by a factor of 3.7 while the Q factor changes by a factor of 2.1 in the weak coupling regime. In the strong coupling case the cavity decay rate changes by a factor of 2.7 while the Q factor changes by a factor of 1.6. Both cases confirm that in case $\eta/\kappa_{FP} > 0.5$ the SE rate change can be higher than the Q-factor change.

In summary, we have demonstrated the real-time, remote all-optical control of the SE rate by more than a factor of three in a coupled PhC cavity system where the control beam is separated more than 20 μm from the target cavity. The results have been interpreted in the framework of CCQED, showing that the SE rate is affected by the change in both the Q-factor and the mode volume. These results open the way to the ultrafast control of the QD-cavity interaction by replacing the thermo-optic tuning with free-carrier injection on the ps time scale.

The authors are grateful to B. Wang, M. A. Dundar, and R. W. van der Heijden for fruitful discussions, and to E. J. Geluk, E. Smalbrugge, and T. de Vries for technical support. This research is supported by the Dutch Technology Foundation STW, applied science division of NWO, the Technology Program of the Ministry of Economic Affairs under project No. 10380, the FOM project No. 09PR2675, and NanoNextNL, a micro and nanotechnology program of the Dutch ministry of economic affairs, agriculture and innovation (EL&I) and 130 partners.

[1] K. J. Vahala, Nature (London) **424**, 839 (2003).
[2] T. Yoshie, A. Scherer, J. Hendrickson, G. Khitrova, H. M. Gibbs, G. Rupper, C. Ell, O. B. Shchekin, and G. Deppe, Narture (London) **432**, 200 (2004).
[3] H. J. Kimble, Nature (London) **453**, 1023 (2008).
[4] J. L O'Brien, A. Furusawa, and J. Vuckovic, Nat. Photon. **3**, 687 (2009).

[5] E. M. Purcell, Phys. Rev. **69**, 681 (1946).

[6] E. Yablonovitch, Phys. Rev. Lett. **58**, 2059 (1987).

[7] Y. Tanaka, J. Upham, T. Nagashima, T. Sugiya, T. Asano, and S. Noda, Nat. Materials **6**, 862 (2007).

[8] T. Tanabe, M. Notomi, H. Taniyama, and E. Kuramochi, Phys. Rev. Lett. **102**, 043907 (2009).

[9] T. Nakamura, T. Asano, K. Kojima, T. Kojima, and S. Noda, Phys. Rev. B **84**, 245309 (2011).

[10] S. Hughes, Phys. Rev. Lett. **98**, 083603 (2007).

[11] S. Vignolini, F. Intonti, M. Zani, F. Riboli, D. S. Wiersma, L. H. Li, L. Balet, M. Francardi, A. Gerardino, A. Fiore, and M. Gurioli, Appl. Phys. Lett. **94**, 151103 (2009).

[12] Y. Sato, Y. Tanaka, J. Upham, Y. Takahashi, T. Asano, and S. Noda, Nat. Photon. **286**, 1 (2011).

[13] M. A. Dundar, J. A. M. Voorbraak, R. Notzel, A. Fiore, and R. W. van der Heijden, Appl. Phys. Lett. **100**, 081107 (2012).

[14] L. C. Andreani, G. Panzarini, and J. M. Gerard, Phys. Rev. B **60**, 13276 (1999).

[15] C. Cohen-Tannoudji, Physica Scripta **T76**, 33 (1998).

[16] We set $Q_{high} = 2 \times 10^4$, $Q_{low} = 2 \times 10^3$, and the dipole is always resonant with one of the coupled modes which has higher Q-factor. For the simulation with multiple FP modes, three equally spaced FP modes with 3 nm separation are taken into account. It should be noted that, in the case of a dipole with fixed energy, the SE rate change in the strong coupling regime will be even higher due to the spectral decoupling between the dipole and coupled mode as the latter is tuned. However, in the experiments described in this work the SE rate of emitters resonant with the coupled mode is measured and the results in Fig. 1 apply.

[17] S. Anantathanasarn, R. Notzel, P. J. van Veldhoven, T. J. Eijkemans, and J. H. Wolter, J. Appl. Phys. **98**, 013503 (2005).

[18] B.-S. Song, S. Noda, T. Asano, and Y. Akahane, Nat. Materials **4**, 207 (2005).

[19] MEEP is developed by the Joannopoulos Research Group at MIT. http://ab-initio.mit.edu/wiki/index.php/Meep

[20] I. Fushman, E. Waks, D. Englund, P. Petroff, and J. Vuckovic, Appl. Phys. Lett. **90**, 091118 (2007).

[21] T. B. Hoang, J. Beetz, L. Midolo, M. Skacel, M. Lermer, M. Kamp, S. Hofling, L. Balet, N. Chauvin, and A. Fiore, Appl. Phys. Lett. **100**, 061122 (2012).

[22] C. Zinoni, B. Alloing, L. H. Li, F. Marsili, A. Fiore, L. Lunghi, A. Gerardino, Yu. B. Vakhtomin, K. V. Smirnov, and G. N. Goltsman, Appl. Phys. Lett. **91**, 031106 (2007).

[23] J. Johansen, B. Julsgaard, S. Stobbe, J. M. Hvam, and P. Lodahl, Phys. Rev. B **81**, 081304 (2010).